

Soft Magneto-Responsive Shape Memory Foam Composite Actuators

Mohammadreza Lalegani Dezaki and Mahdi Bodaghi*

Soft magnetic composites are exceptional because they can be controlled remotely, move quickly, conform to hard things, and interact with people safely. However, even with all these features, magnetic elastomers suffer a lack of stability due to the high softness of the elastomer. This issue affects their controllability and repeatability. This article introduces a novel conceptual design of magneto-responsive shape memory polyurethane (SMP) foam composites with high stability and reversibility. The fabrication technique is based on the silicone resins filled with strontium ferrite magnetic particles and a thin SMP foam placed onto one side. Material properties, room-temperature shape recovery features, and magnetization conditions necessary for the process are determined by experimental studies of composite actuators. As a result, a workable, light, stable, soft composite gripper with programmable magnetic patterns is created, which can carry out activities like grabbing, holding, and moving objects in horizontal and vertical directions when a low magnetic field is applied. The SMP foam increases the contact surface and decreases the weight by up to three times providing better stability compared to the magnetic elastomer without SMP foam. The shape-recoverable gripper with a small contract area can lift objects eight times heavier than its weight.

contrast to conventional robots made of rigid materials. With this kind of robotics, a variety of unique soft mobile platforms, manipulators, and other structures have been developed that can carry out a variety of increasingly complicated activities, including wearable robotics, object manipulation, and mobility over uneven terrain.^[3–6] These objectives are driven by a variety of actuation concepts, including tendon and pressure actuation as well as reactions to different stimuli (such as magnet, humidity, temperature, and light).^[7,8] Elastomeric soft actuators continue to get more complicated, and roboticists push the limits of soft robotics in order to create actuators and sensors with more advanced designs. Soft robots employ clever solutions based on smart materials that can sense and act in order to further simplify the design and boost functionality.^[9–11]

Magnetically responsive actuators are particularly intriguing among the several conceivable types of devices and actuation modes since they are quick, contactless, and powered by magnetic fields that may be


used safely around people.^[12–15] For minimally invasive medical devices, contactless control makes it possible to operate untethered equipment in small places.^[16–18] Creating simple things in the continuous attempts to design devices with complicated output motion powered by a simple single input, magneto-responsive is also a viable strategy. Kim et al.^[19] have demonstrated that when a magnetic actuator is activated by an external magnetic field, soft objects with controllable local magnetization patterns may perform sophisticated motions like crawling, rolling, and leaping. The creation of soft materials that are magneto responsive has previously involved the use of several types of magnetic particles such as NdFeB.^[20,21]

Strontium hexaferrite (SrFe₁₂O₁₉) exhibits the hard magnet properties of NdFeB while simultaneously being susceptible to magnetization at relatively low magnetic fields, making it an intriguing replacement for the magnetic particles now in use.^[22] Carpenter et al.^[23] developed a silicone-based composite actuator containing SrFe₁₂O₁₉ magnetic particles. A range of functional soft actuators that can be remotely controlled by an external magnetic field is created using their particle-filled silicone resins. Qi et al.^[24] provided a shape-programming technique that created the necessary magnetic moment and actuating magnetic fields for magneto-active soft materials with rapid, reversible, programmable, and stable shape transformation capabilities. By

1. Introduction

Contrary to conventional robots, soft robots attempt to mimic the inherent softness, suppleness, and adaptability that traditional robots are unable to achieve without direct control of motor function.^[1] In order to simplify machines and get closer to biology's mechanical capabilities, the discipline of soft robotics employs compliant structures.^[2] Soft robots can navigate surroundings by altering their shape and size while applying modest contact pressures and avoiding damage from rapid contact, in

M. Lalegani Dezaki, M. Bodaghi
 Department of Engineering, School of Science and Technology
 Nottingham Trent University
 Nottingham NG11 8NS, UK
 E-mail: mahdi.bodaghi@ntu.ac.uk

 The ORCID identification number(s) for the author(s) of this article can be found under <https://doi.org/10.1002/mame.202200490>

© 2022 The Authors. Macromolecular Materials and Engineering published by Wiley-VCH GmbH. This is an open access article under the terms of the Creative Commons Attribution License, which permits use, distribution and reproduction in any medium, provided the original work is properly cited.

DOI: 10.1002/mame.202200490

printing various magnetic structural components, this technique was used to program the magnetic moment in the soft matrix. The high-performance deformation of magneto-active soft materials was made possible by the flexible matrix and soft magnetic 3D printing filament. Ju et al.^[25] developed a direct magnetization technique based on pulsed high magnetic field focusing, allowing for millisecond-scale precision and flexible programming of the local magnetization distribution after creation.

Despite numerous studies on elastomeric magnetic actuators, they still suffer a lack of stability and controllability in the system due to the low stiffness of elastomers. Hence, using stiffer material in the system helps increase actuators' stability.

Due to its continuous structure, low modulus, compressibility, and capacity to readily buckle, foams are an alternate material that hasn't been completely investigated but could provide advantages to magnetic actuators. Foams are particularly intriguing as structural components in various applications^[26,27] because they can be manufactured from several solid materials with varying degrees of stiffness and extensibility. Li et al.^[28] provided the first material model for syntactic foams based on shape memory polymers (SMPs).^[29] Li et al.^[30] updated the model through a series of tests and proposed a 1D model to forecast the behavior of SMP foams under compressive stress. Xu et al.^[31] reformed and enhanced Boyce's thermo-visco-elastic constitutive model^[32] to predict the thermo-visco-plastic response of the SMP foams. Also, Jarrah et al.^[33] expanded the rheological thermo-visco-plastic Arruda-Boyce model for SMP foams. However, in their study, the chosen model was used to examine the super-elasticity of SMP foams under compression at room temperature.

Foams undergo a significant mechanical change when turned into foam, usually becoming substantially more compressible.^[34] Foams exert little stress on their surroundings since it is lightweight and soft structurally. Similar to this, low-force actuators may be used to deform foam robots. The open-cell foam may be compressed for small-volume robot packaging during transportation, and as the vacuum does not affect its resting shape, it is appropriate for tasks like inspecting a fragile antenna on the outside of a spacecraft.^[35] In addition, strawberries might be harvested autonomously by foam robots without being crushed. Murray et al.^[36] used foam that buckled in soft pneumatic actuators. By using elastomer foam as the mechanism for cardiac compression, the research proposed the first step toward a pneumatically driven, patient-specific direct cardiac compression design. Donatelli et al.^[37] introduced SquMA Bot which was a soft robot with caterpillar influences. The body of the robot was mostly made of soft viscoelastic foam and was moved using a motor-tendon system using shape memory alloys. Also, Kastor et al.^[38] developed an inexpensive motor tendon-actuated soft foam robot. The technique created a structure that could withstand substantial deformations (up to 70% strain) by using a castable, light, and readily compressible open-cell polyurethane foam. Meanwhile, about how to construct and use SMP foams in magnetic soft actuators, there is currently very little public information.

Previous research on foams in robotics has either concentrated on soft foam robotic components or on the use of stiff foam structural elements in situations where weight was particularly essential. However, the potential of SMP foams integrated with elastomeric magnetic actuators has not been explored yet. In this

work, for the first time, a stable, reversible, light composite actuator with flexible SMP foam and magnetic elastomer components is developed. A lightweight soft actuator powered by permanent magnets and a low magnetic field and molded from SMP foam and the magnetic elastomer is introduced. The primary objectives of this study are to propose a conceptual design, to completely detail the manufacturing process utilized to create this kind of soft shape-memory actuators, and to outline certain key design parameters. The creation of straightforward production procedures may be helpful to make actuators with a variety of applications. The accessibility of magnetization equipment is frequently a limiting issue that is solved in this research. It is expected that the model and solution techniques would serve as a helpful method to produce lightweight magneto-responsive actuators to operate in horizontal and vertical directions with high stability and small contact area. The structure of this work is as follows. The mechanical properties of SMP foam are studied. Also, information about room-temperature shape recovery features of the hyper foam is presented. The manufacturing procedure of composite magnetic elastomers with integrated SMP foams is also discussed. Finally, the application of the developed actuator is evaluated accordingly.

2. Experimental Section

2.1. SMP Foams

2.1.1. SMP Foams Properties

The SMP foam from SMP Technologies Inc. was taken into account for the experiment as a soft actuator in this work. The new feature of this SMP foam was that it recovered its original shape faster at room temperature compared to other foams. The dynamic $\tan \delta$ of this foam was more similar to human skin with a value of 0.4–0.6 based on the supplier catalog. Also, SMP foam had Young's modulus of 39 MPa during rest time while it increased to 135 MPa when it was compressed. This foam's most significant benefit was that, in addition to having great biocompatibility characteristics, it can be molded into any complicated shape without the need for additional procedures. Scanning electron microscopy (SEM) (JSM-7100F LV FEG SEM machine) was used to evaluate the microstructure of SMP foam and microstructure features.

2.1.2. Fatigue and Shape Recovery of SMP Foams

It should be noted it was vital to decrease the timing of shape recovery of soft actuators. Also, achieving a stable soft actuator was highly effective to increase precision and repeatability. Hence, the reversibility to the original shape was crucial for smart actuators. The reversibility of SMP foam was investigated to check the room-temperature shape recovery here. The tests were conducted to evaluate the time that the foam took to go back to its initial form using bending and compression tests. The permanent shape of SMP porous materials was measured and could have an impact on the material's performance. Hence, the change recovery through compression was measured during the compression

test. ElectroForce 3200 from TA Instrument was used to conduct the fatigue and shape recovery test. A rectangular cubic shape foam was cut with the size of 18 mm in length, 18 mm in width, and 10 mm in thickness. The density of the cut foam was 0.005 g cm^{-3} . The load cell of 450 N and the frequency of 1 Hz were used to compress the sample. Two hundred cycling loads were applied for 35% and 60% strains at room temperature. Data were recorded to investigate the shape recovery after these 400 cycles on one sample. Moreover, shape recovery time while the foam was bent was investigated as well. A foam with the size of 10 mm in width, 70 mm in length, and 5 mm in thickness was cut. A weight of 1 kg was put on the sample while it was bent. After 5 min the load was removed, and the time of shape recovery was recorded accordingly. A high-speed camera was used to record the shape recovery of the SMP foam.

2.1.3. Mechanical Properties of SMP Foams

Shimadzu AG-X plus machine was used to conduct the quasi-static mechanical testing and TRViewX recorded the data. A cube of SMP foam with the size of 50 mm in length, 50 mm in width, and 10 mm in thickness was used for the compression test. The density of the cut foam was 0.05 g cm^{-3} . A double-sided tape was used to hold the sample during the test. The compression test was conducted using a 1 kN load cell. The test was performed up to 30% strain using 1 mm min^{-1} displacement rate.

2.2. Magnetic Composite Elastomers

2.2.1. Magnetic Particle

Due to the flexibility of the suggested manufacturing method, there was a wide range of options for the chemical make-up, size, and shape of the magnetic particles used in the formulation. Studying the magnetic characteristics, mechanical characteristics, and deformation of soft foam composites made with various types of particles allowed to investigate this design space. Bimodal particle size distribution strontium ferrite, $\text{SrFe}_{12}\text{O}_{19}$, (UF-S2) from DOWA Electronics Materials was examined accordingly. SEM was used to examine the microstructure of particles. It had an average particle diameter of $1.3 \mu\text{m}$ and 3.58 g cm^{-3} compressed density. This powder was appealing to produce soft actuators since it might be magnetized using composites containing strontium ferrite particles at relatively low magnetic fields and biocompatibility.^[39,40]

2.2.2. Magneto-Responsive Foam Composites

Making magneto-responsive soft actuators just required combining magnetic particles with a two-part silicone resin and molding the resultant viscous paste. An IKA MINISTER stirrer was used to combine the UF-S2 particles with the Ecoflex 00–30 silicone resin (part A and part B) from Smooth-On-Inc until a smooth, viscous paste was produced. Bimodal strontium ferrite ($\text{SrFe}_{12}\text{O}_{19}$) particles made up 70 wt.% of the composite paste used to make all of the films. By measuring the magnetic flux density on the

surface of the samples in the out-of-plane direction, the magnetic characteristics of the composite films were measured.

The paste was then molded to produce films of 60 mm in length, 10 mm in width, and 2 mm in thickness by casting into 3D printed polylactic acid (PLA) molds using the fused deposition modelling (FDM) process.^[41] The resin became more viscous due to the development of a percolating network between the particles, which also hindered the final paste from freely flowing (see Figure 1a). Therefore, in order to fill the molds and provide a clean surface finish, the paste must be compressed throughout the casting process. The presence of air bubbles could not be prevented due to the high paste viscosity, although they had no discernible impact on the final characteristics of the composites.

The magnetic silicone composite films were too soft, and they did not have enough stability. Hence, it was vital to maintain the position of the actuator without changing the stiffness and weight. To achieve a stable soft actuator, a piece of SMP foam with a thickness of 3 mm was cut. The manufacturing procedure was similar to composite films. The foam was placed on the top of silicone with magnetic particles during the curing time as shown in Figure 1b. Mold was 3D printed using FDM and magnetic particles with two-part silicone resins were poured into the molds. The magnetic viscous was poured until a thickness of 2 mm elastomer was achieved. Then, the SMP foam strips were placed and pressed. The composite was shaped and then allowed to cure for at least 4 h at room temperature in the fields of commercial neodymium magnets (see Figure 1c). The size of the final sample was 60 mm in length, 10 mm in width, and 5 mm in thickness. A magnetic elastomer with the same size as the final composite SMP foam actuator was produced. Alternatively, a magnetic elastomer with the size of 60 mm in length, 10 mm in width, and 2 mm in thickness without SMP foam was produced (see Figure 1d). A comparison was made between samples to investigate the effect of SMP existence in the magnetic elastomer in terms of stability and weight.

Due to the ability to employ foams for the core, the actuators were especially well suited for creating actuator structures with shape recovery capabilities. To magnetize the soft actuator with or without SMP foam, an arrangement was used. In order to obtain a uniform, out-of-plane magnetization, square neodymium magnets were used. The permanent magnet was positioned on one side of the mold and was used to magnetize the soft actuators during the curing. At the end of each film, there was one square magnet ($15 \times 15 \times 8 \text{ mm}$, N42, Magnet Expert Ltd) to magnetize the soft composite. Greater magnetization was attained by samples magnetized during curing as the result of the particles aligning with their easy axis along the applied field.^[23]

2.2.3. Functional Soft Actuator

For pick-and-place, gripping, and moving operations as well as 3D objects with remote control morphing capabilities, magneto-responsive soft materials can be employed as actuators and rapid, untethered robots. The aim was to achieve the thinnest and soft actuator using magnetic elastomer and SMP foam. The design allowed for the development of an actuator based on requirements. The four-arm soft grippers were operated manually using neodymium magnets in trials. Small magnets were used to

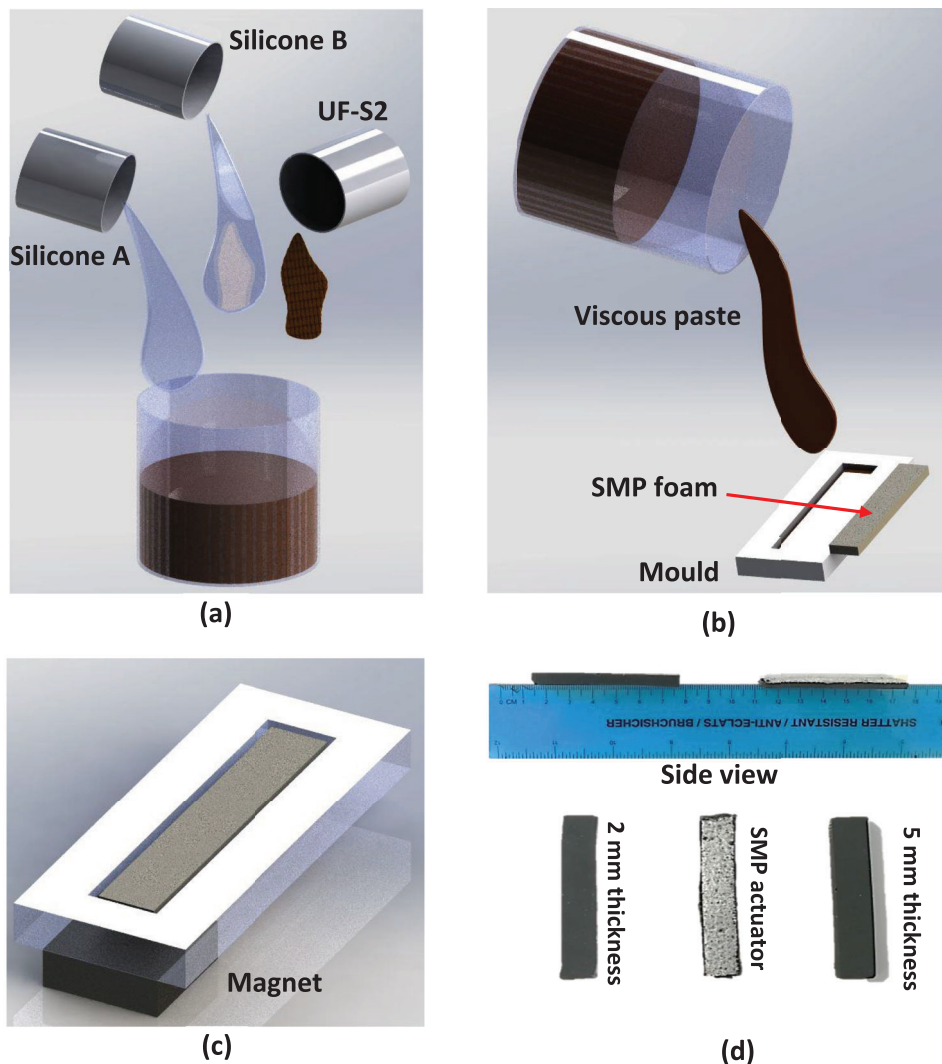


Figure 1. The manufacturing, magnetization, and activation of magneto-responsive foam composite. a) By combining the magnetic powder with a two-part Eco-flex silicone resins, soft objects are created. b) To construct actuators with precise geometries, the viscous paste is cast into the 3D-printed mold. c) A neodymium magnet is used to magnetize the film by positioning them in specified locations during the curing process. d) Cured composite films with and without SMP foam.

magnetize the four-arm gripper on one side of the gripper. Grippers hanging beneath a permanent magnet (60 mm diameter and 5 mm thick N42, Magnet Expert Ltd) were used to quantify gripper movement and lifting. The design and assembly of the actuator are shown in **Figure 2**. The size of each arm was 25 mm. The middle of the actuator was just a magnetic elastomer without SMP foam. The magnets attracted the magnetic paste to the end of each arm. Small 3D-printed samples with various shapes were developed to be lifted by the actuator. The design was developed in SolidWorks and molds were printed using PLA material. The strip foams with a thickness of 2 mm were placed into the mold and the viscous paste was poured into the mold. A plate was placed on the top of the mold and pressed for 4 h until the silicone was cured. By altering the distance between the magnet and the gripper, the magnetic field that was applied was regulated. By overlaying the magnetic fields with a magnet that can be moved manually, the grippers can open and close. By mounting the ac-

tuators vertically or horizontally, their ability to be magnetically controlled to actuate the magneto-responsive composite foams was investigated.

2.2.4. Magnetic Measurement and Deflection

A physical property measurement system (PPMS; Quantum Design) was used to monitor the hysteresis loops of magneto-responsive composites at 300 K and a rate of 2.5 mT s^{-1} . The bending deflection of free-hanging cantilever foam composite beams was examined under the presence of an external lateral magnetic field with different distances between the permanent magnet (50×50×5 mm thick N42, Magnet Expert Ltd) and foam actuator to evaluate the film's responses. The experiment was conducted when the soft composite actuators were exposed to an external magnetic field. The magnetization patterns were made

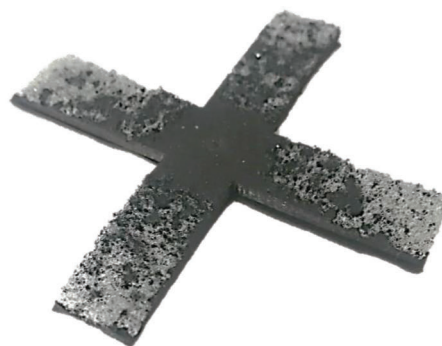
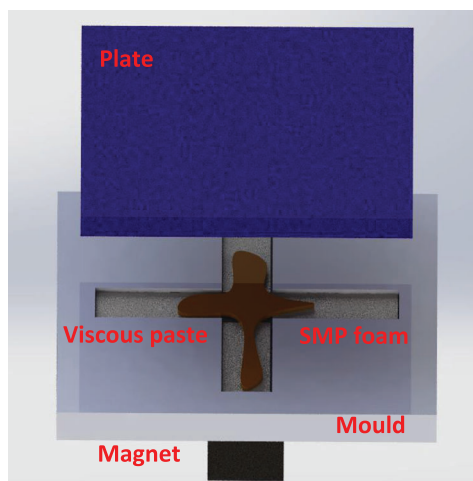


Figure 2. Magneto-responsive composite actuators as a gripper.

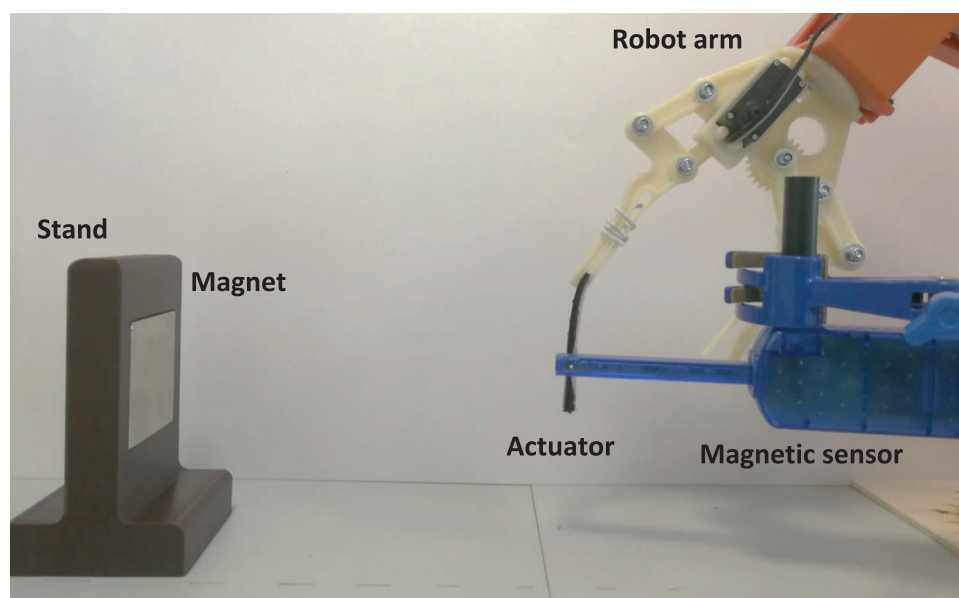


Figure 3. The test setup for measuring the responsiveness of the composite actuator.

during the manufacturing procedure to control their motion. A neodymium magnet parallel to the direction of the film was placed at different distances while the film was hanging vertically (see **Figure 3**). A magnetic field sensor with a probe from Pasco with a resolution of 0.01 G was used to detect the magnetic strength of the neodymium magnet along two perpendicular axes using 10 Hz frequency. PASCO Capstone was used to record the magnetic strength of the permanent magnet. The distance of the magnet was changed to record the bending and deflection of the composite actuator. Also, a portable Gaussmeter from RS pro was used to test the magnetic flux density. Soft actuators' trajectory paths were recorded by PASCO software to measure bending angles and deflection.

2.2.5. Mechanical Characterization

A universal mechanical testing device (Shimadzu AG-X plus machine) was used to assess the composites' mechanical properties. Three dog-bone shape silicone samples (Ecoflex 00–30) and three samples with 70 wt.% magnetic particles were molded in 3D printed samples in accordance with ASTM D412 with a gauge length of 33 mm.^[42] The test was conducted to evaluate the stress differences with and without magnetic particles. **Figure 4a,b** shows the molded samples and tensile test procedure accordingly. The samples were clamped between jaws and 500 mm min⁻¹ displacement rate was applied to the dog-bone samples.

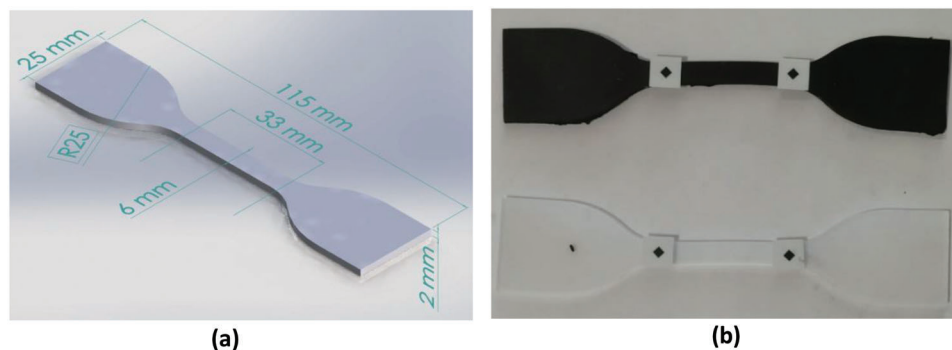


Figure 4. a) 3D schematic of the dog-bone shape sample with its geometries. b) The dog-bone samples with and without UF-S2 particles for tensile test

3. Results and Discussion

3.1. SMP Foam Characteristics

Figure 5a depicts the microstructure of the SMP foam construction with porosity inside them. The microstructure of the foam is made up of many pores that range in size from 1 mm to 100 μm . Also, there are tiny pores inside the microstructure of the foam. In this model, the volume percentage of the matrix materials should be taken into account since these pores decrease the mechanical characteristics of the foam. The three major stages of the stress–strain curve for SMP foam under compressive loading are linear elastic, plateau, and densification. Morphological properties of the ligaments, including density, anisotropy, polydispersity, and foam cells, heavily influence the foam response.

The experimental stress–strain curve for SMP foam is investigated accordingly. The foam model is subjected to maximum strains. The material exhibits various characteristics under the compression load. The SMP foam exhibits a super-elastic hardening–softening–hardening response. The plateau area, or softening section, is caused by the local buckling deformation and rupture of the cell structures. The beginning of the densification regime, which occurs when the stress grows significantly, marks the end of the plateau regime. **Figure 5b** demonstrates the key characteristics of SMP foams, including elastic and super elastic behaviors, and softening plateau up to 30% strain. By applying the load on the SMP foam, the distances between pores decrease that leads to a higher density well-known as densification. By increasing the load, the foam is compacted and the stiffness of the foam increases accordingly.

The mechanical behavior of the SMP foam during the loading–unloading cycle are shown in **Figure 5c,d** for 30% and 60% maximum strains, respectively. The test speed is 1 Hz for both procedures. According to stress–strain experimental data, the SMP foam dissipates and absorbs energy via the hysteresis loop. The pores inside the foam are compacted in order to bear the applied compressive load. The foam’s structure experiences a significant distortion in the super-elastic deformation range with the roughly constant compressive force. When the structure is unloaded, the compacted pores recover to their original size which is resulted in returning foam to its original shape after a few seconds (see **Figure 5e**). It shows the capabilities of SMP foam in terms of energy absorption and shapes memory recovery after unloading at room temperature. As an example, the reversibil-

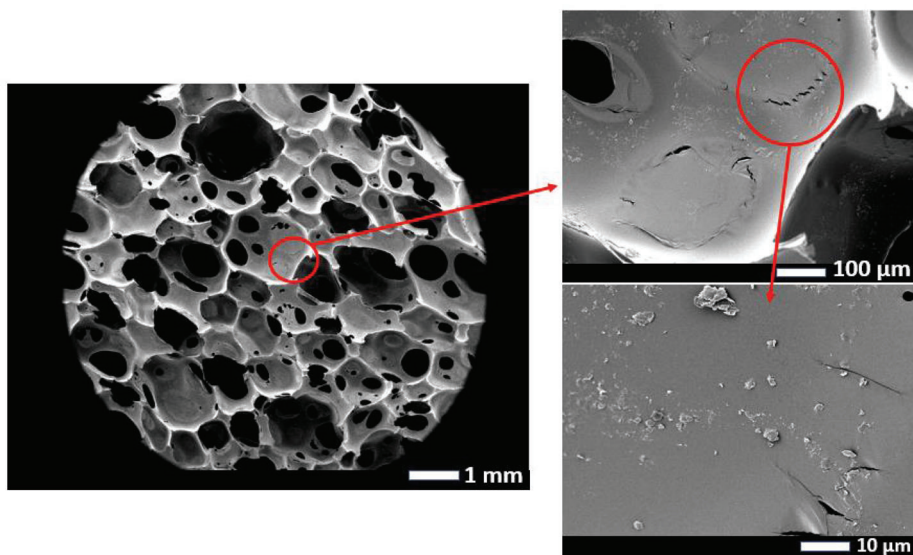
ity of the SMP foam with 60% maximum strain starts when it is unloaded. As the cyclic loading is done fast, the SMP foam does not have time enough to fully recover to the original shape (see part 4 of **Figure 5e**), and therefore the next cycle is applied to the partially compressed foam. The SMP foam can fully return to its original shape in a quasi-static test mode.

The bending recovery time is also shown in **Figure 5f**. After removing the weight, the time is recorded accordingly. The sample goes back to its initial shape after 8 s. Results show that shape recovery is also happening in bending as well. It should be noted the bending of SMP foam in this study is less than a minute. Hence, the shape recovery time is fast enough for lightweight reversible actuators. The results indicate the SMP foam has high capability in terms of shape recovery and energy absorption. Hence, by applying silicone elastomer to one side of the SMP foam as discussed, the actuator’s performance is investigated accordingly.

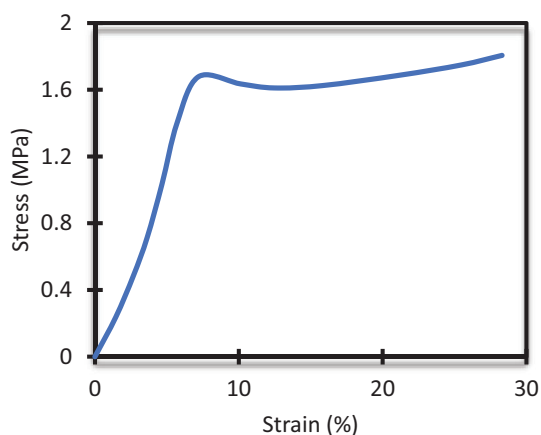
3.2. Magneto-Responsive Composites

Strontium ferrite disk-shaped particles with bimodal size distributions are examined. The chemistry and morphology of UF-S2 were investigated in [43–45] and are not reported in this work for the sake of brevity. For more details, one may refer to Ref. [43–45]. A blend of 3.0 and 0.8 μm particles makes up the bimodal $\text{SrFe}_{19}\text{O}_{20}$ particles (see **Figure 6a**). UF-S2 particles are discovered to create a composite when added to silicone resin following the polymerization of the resin mixture as shown in **Figure 6b**. To assess the magnetic response of the particle-filled silicones, magnetization curves are employed. The magnetic moment under external magnetic fields is up to 3000 Oe, which is a low value generally attained. The magnetization moment of the composite film without SMP is shown in **Figure 6c**. According to the experimental findings, magnetic elastomer magnetizes to remanent levels of 30 emu g^{-1} . The magnetic dipoles of UF-S2 particles are more easily directed when magnetic fields are applied, and they can be retained when the fields are removed, according to the strong remanent magnetizations. The external field must be stronger than the material’s coercive magnetic field in order to permanently orient magnetic dipoles in a certain direction. [23]

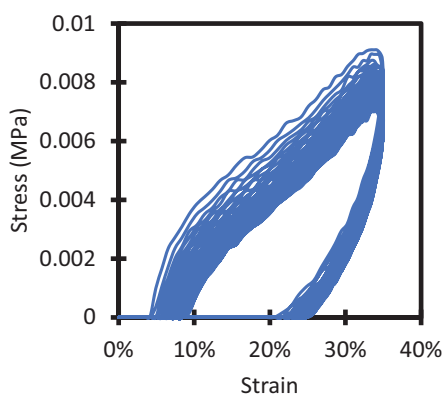
The obtained results demonstrate that the elastomer composite operates in a manner similar to hard magnets, which exhibit a significant hysteresis response and a high coercive field of 3000 Oe. Magnetization during silicone curing shows high



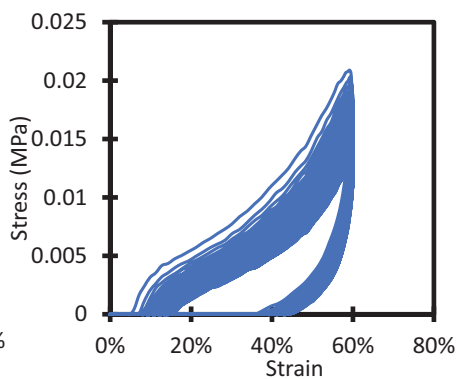
(a)



(b)

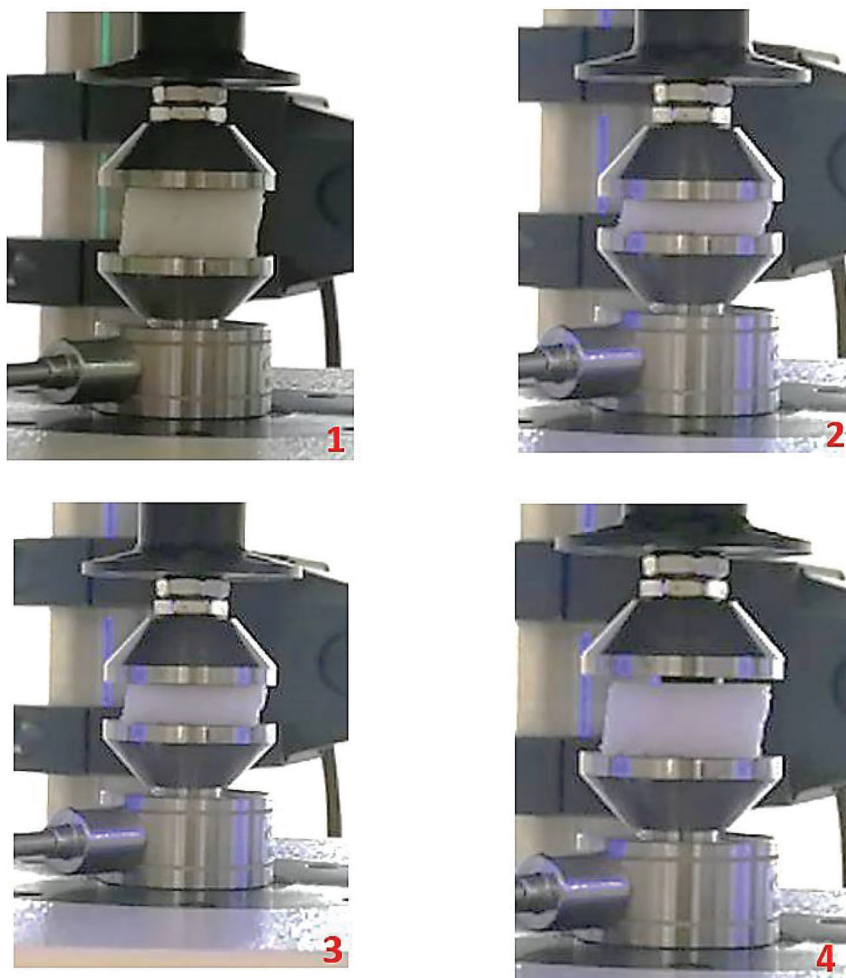


(c)

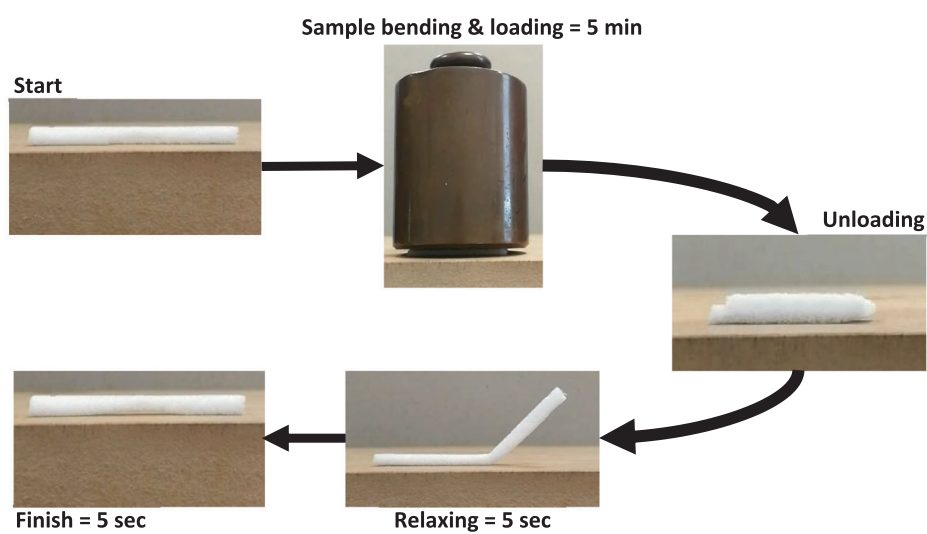


(d)

Figure 5. a) The presence of pores with various sizes in SEM images of SMP foam. b) Stress-strain graph of cut foam with the size of 50 mm in length, 50 mm in width, and 10 mm in thickness. c) Cycling loading of SMP foam with 30% maximum strain. d) Cycling load of SMP foam with 60% maximum strain. e) The steps of load/unload of SMP foam with 60% maximum strain rate for cycle 100. f) The bending shape recovery and reversibility of SMP foam using 1 kg load.



(e)



(f)

Figure 5. Continued

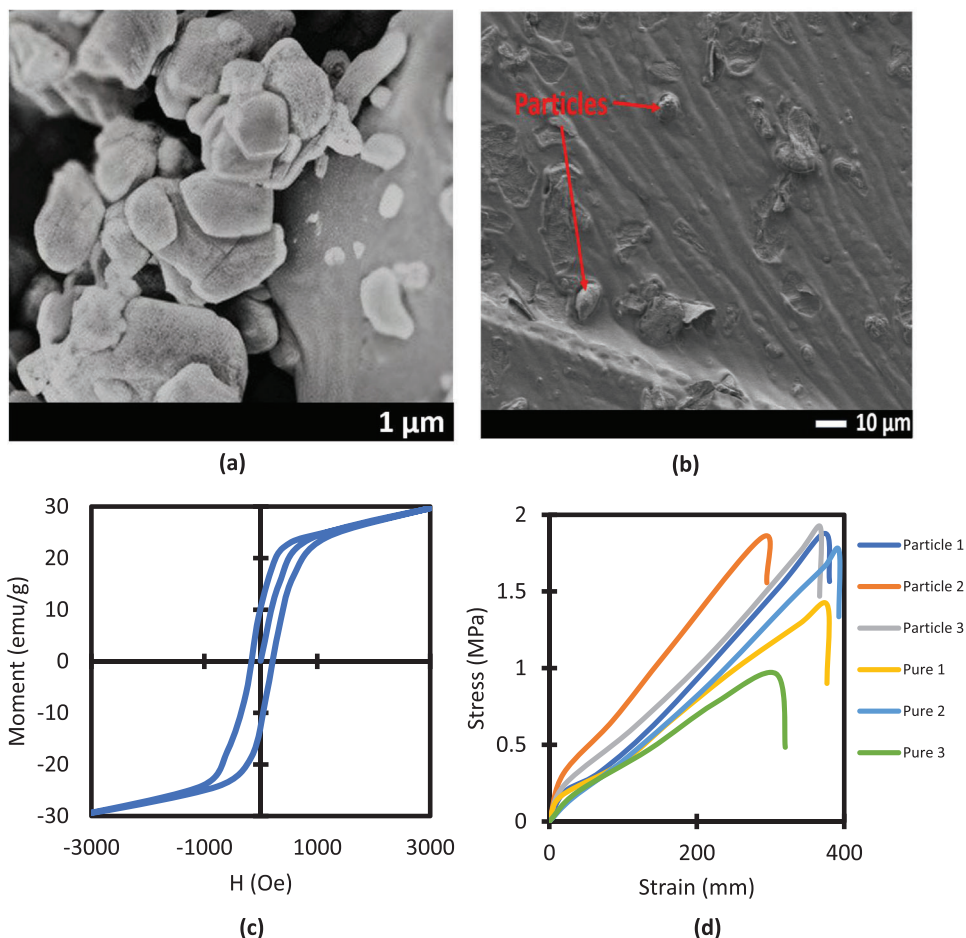


Figure 6. a) The form and size distribution of the UF-S2 particles are visible in the SEM image. b) Composites are made with UF-S2 magnetic particles as seen through the SEM image. c) Cyclic magnetization curve with H-field rising progressively from -3000 to 3000 Oe for silicone composites. d) Tensile test graph of silicone composite samples with and without magnetic particles.

remanent magnetization. This demonstrates that while the resin is still being totally cured, the particles align with their simple long axis parallel to the applied magnetic field. If the driving field is kept within the range of ordinary permanent magnets, the composite films may be repeatedly activated without magnetization loss. Also, the results of tensile tests show that silicone films made with strontium ferrite particles outperform by having high compliance compared to pure silicone (see Figure 6d). This means that the composite films with UF-S2 particles are stronger due to the existence of UF-S2 particles compared to the dog-bone pure silicone samples.

The next comparison study shows how the foam increases the magnetic elastomer's stability while reducing the strip's weight. Composite films with 2 mm, 5 mm, and SMP foam are investigated accordingly. Figure 7a–c reveals that by holding the strips horizontally, the magnetic elastomer with SMP foam has the same stability as the elastomer with 5 mm thickness without SMP foam. However, the weight of a strip with foam is 1.55 g while a strip without foam is 4.45 g within the same size. Also, by decreasing the thickness of the elastomer to 2 mm without foam, the film does not have enough stability. Thus, the SMP foams increase the stability of the magnetic elastomer. This is useful in

actuators to have better accuracy and repeatability compared to the other samples. Also, reducing weight, in this case, is effective in terms of material wastage and having lighter products.

The local flux density, which changes linearly with the soft material's magnetization, is mapped out. As shown in Figure 8a, the concentration of UF-S2 particles is higher at the end of the composite SMP film compared to other regions. The negative value is due to the magnetization of the actuator during the curing procedure. Red dots on the sample in Figure 8a shows the areas where flux density is measured. Due to the natural concentration of magnetic flux near the edges of the magnetizing magnet, the end of the film exhibits a little stronger magnetization than the rest of the film. Hence, the end of the film is actuated by a small magnetic field compared to other areas.

A low magnetic strength affects the composite film accordingly. The actuation of our composite films is already conceivable with external fields that are one order of magnitude lower than this top demagnetization limit, according to deflection measurements (see Figure 8b). Due to the high force generated in response to the magnetic field, we have decided to strongly clamp one side of the film. As shown in Figure 8c, a bi-directional actuator is conducted due to the existence of a cubic magnet at the

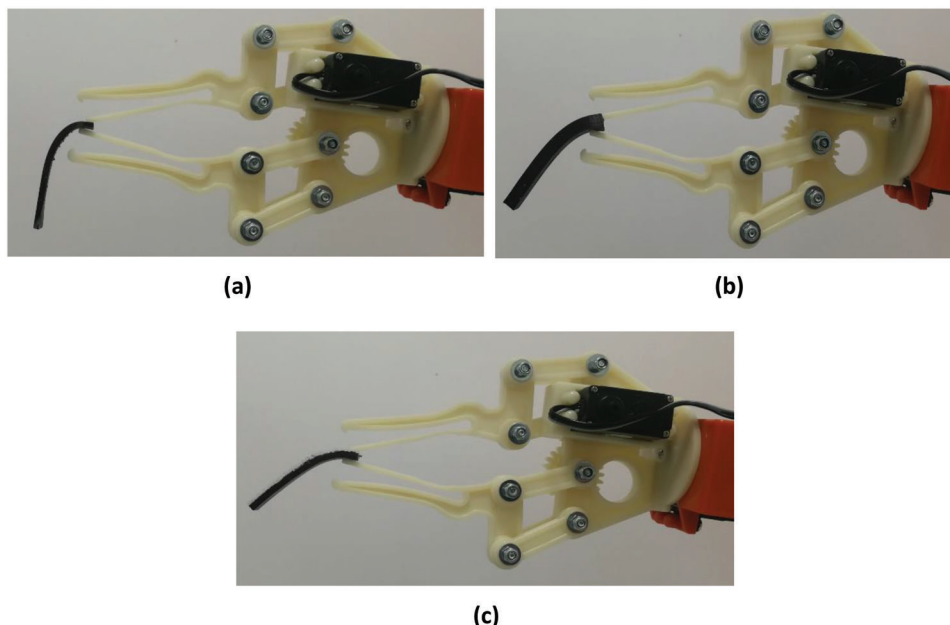


Figure 7. a) Magnetic elastomer with 2 mm thickness. b) Magnetic elastomer with 5 mm thickness without SMP foam. c) Magnetic elastomer with 2 mm thickness and 3 mm thick SMP foam.

end of the foam actuator. This happens because the magnetic domains at the end of strips are orientated in opposition to one another. This pattern develops as a result of the strips being exposed to the closing flux lines that link the opposing poles of the magnet pair placements. In contrast to the magnetic field produced at the end of the composite actuator, the magnetic field along these closing lines is orientated in the opposite direction. The observed magnetic and mechanical qualities are reflected in the composite foam films' reaction to an external magnetic field. Films containing strontium ferrite exhibit remarkable magneto-responsiveness in the presence of magnetic fields because of their high compliance and magnetism.

The magnetic field strength is also recorded during the procedure. The axial and perpendicular strength of the magnetic field increase by decreasing the magnet distance. At 5 cm, 17 mT strength and -3.5 mT are recorded for axial and perpendicular, respectively (see Figure 8d). The negative value of strength is due to the opposite direction of the magnetic field. Also, by rotating the magnet, the values of -15 and 3 mT are achieved at different distances (see Figure 8e). As shown in Figure 8f,g, the trajectory paths of composite actuators show how the magnet attracts and repulses the composite actuator at different distances. At 15 cm, the magnet starts to repulse or attract the actuators.

The maximum angle of 37° for attraction and 30° for repulsion are conducted at 5 cm distance for SMP foam actuator, respectively (see Figure 8h). The actuator with 2 mm thickness has the highest bending angle and deflection among others in both attraction and repulsion with low magnetic strength. However, by removing the magnet, the structure is not stable enough when it goes back to its initial shape. Also, by removing the magnet quickly the actuator film without SMP starts to vibrate and becomes unstable. Meanwhile, the composite SMP foam actuator goes back to its initial shape in less than a second without the

instability that the thin elastomer has. Also, SMP foam actuator shows better performance compared to the actuator with 5 mm thickness (see Figure 8i). This means SMP foam is highly effective in changing the magnetic elastomer into a better actuator. Also, this method can be applied to different designs and shapes based on requirements and magnetic field strength.

3.3. Functional Grippers

The new SMP foam composite with magnetic elastomer developed in this study is employed to design cross-shaped smart functional grippers as described in this section. A bolt and nut are used in the middle of the actuator to hold it properly. The produced actuator with a weight of 3 g is stable enough when it is held vertically or horizontally as shown in Figure 9a. This allows the actuator to grasp the object in both directions easily. The end arms of soft composite actuators are attracted and driven back using the neodymium magnet. The magnet attracts the arms when the particles have an opposite alignment with the field (see Figure 9b).

In both open and closed conformations, the gripper's arms expand when magnetic domains are aligned in the same direction (see Figure 9c). Thus, the magnetic field is strong enough to actuate the gripper in terms of the arm's opening and closing. The foam which is attached to the magnetic elastomer makes the actuator's structure stable. This means the actuator can overcome gravity without issues. Also, the shape recovery of actuators is faster, and deformation and twisting are not happening due to the existence of the SMP foam. Figure 9d shows the behavior of the composite actuator with different magnetic field strengths.

The soft gripper is used to lift things along the vertical direction that are substantially heavier than the actuator itself because

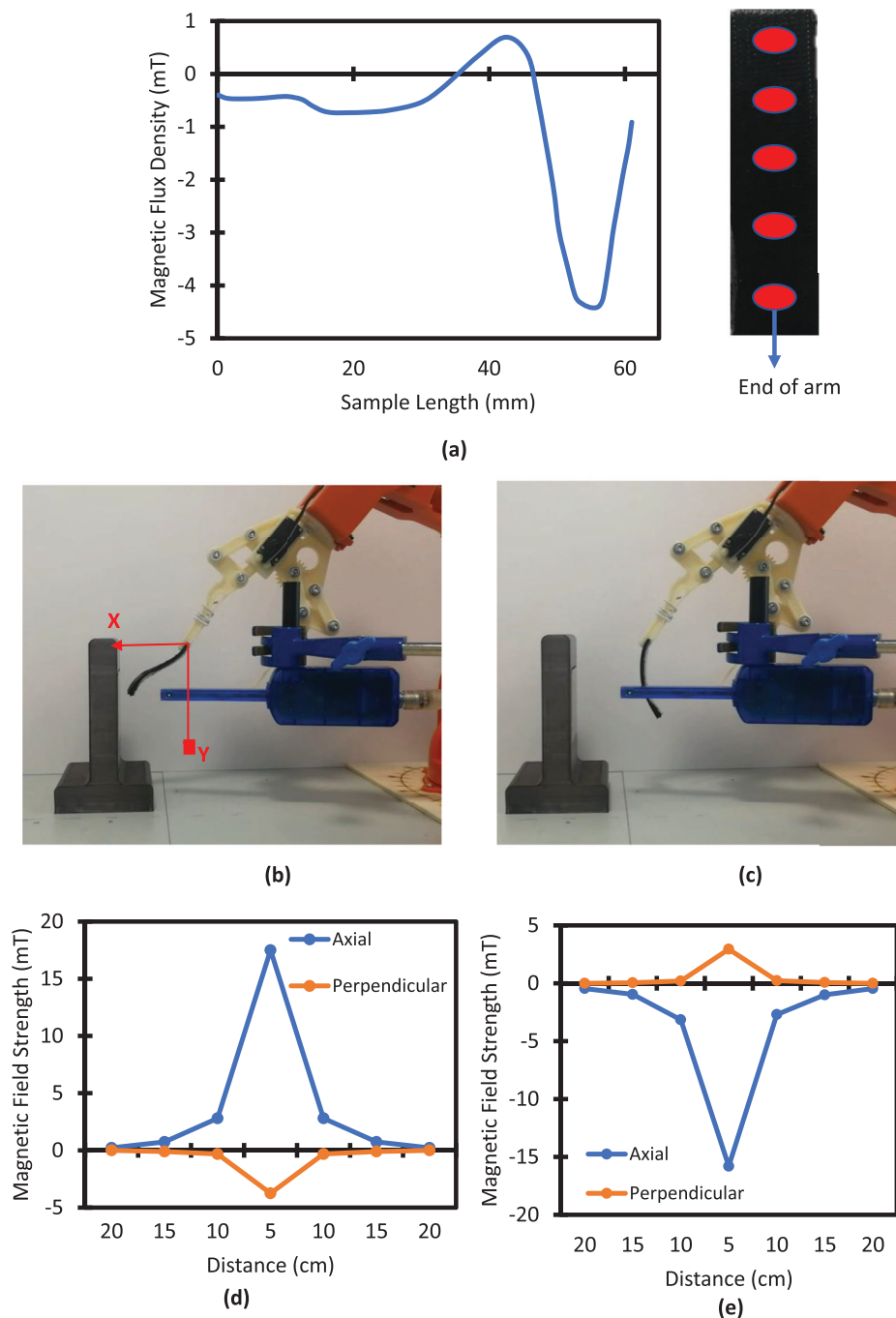


Figure 8. a) Magnetic flux density of composite SMP actuator with varying concentrations of UF-S2 particles. b) Deflection of the SMP actuator using a permanent magnet. c) Bi-directional composite actuator by rotating magnet. d) The axial and perpendicular magnetic field strength of the permanent magnet at different distances. e) The axial and perpendicular field strength of the rotated permanent magnet at different distances. f,g) The trajectory path of the composite actuator with SMP foam using a magnet at different distances. h,i) Bending angle of the deflected composite actuators at different distances.

of the contact force and surface area with the chosen object and the SMP foam of the extended arms in the closed position. Friction at the point of the contact surfaces between the SMP foam and the surface of the object makes it possible for such lifting and holding objects. Gravity-driven sliding of the object through the

extended gripper arms is slowed down by frictional forces. The bioriented gripper is shown in **Figure 10a**. By rotating the permanent magnet, the gripper's arms are driven back and they release the object faster. Then, the arms go back to their initial position quickly. The gripper is capable of holding different weights and

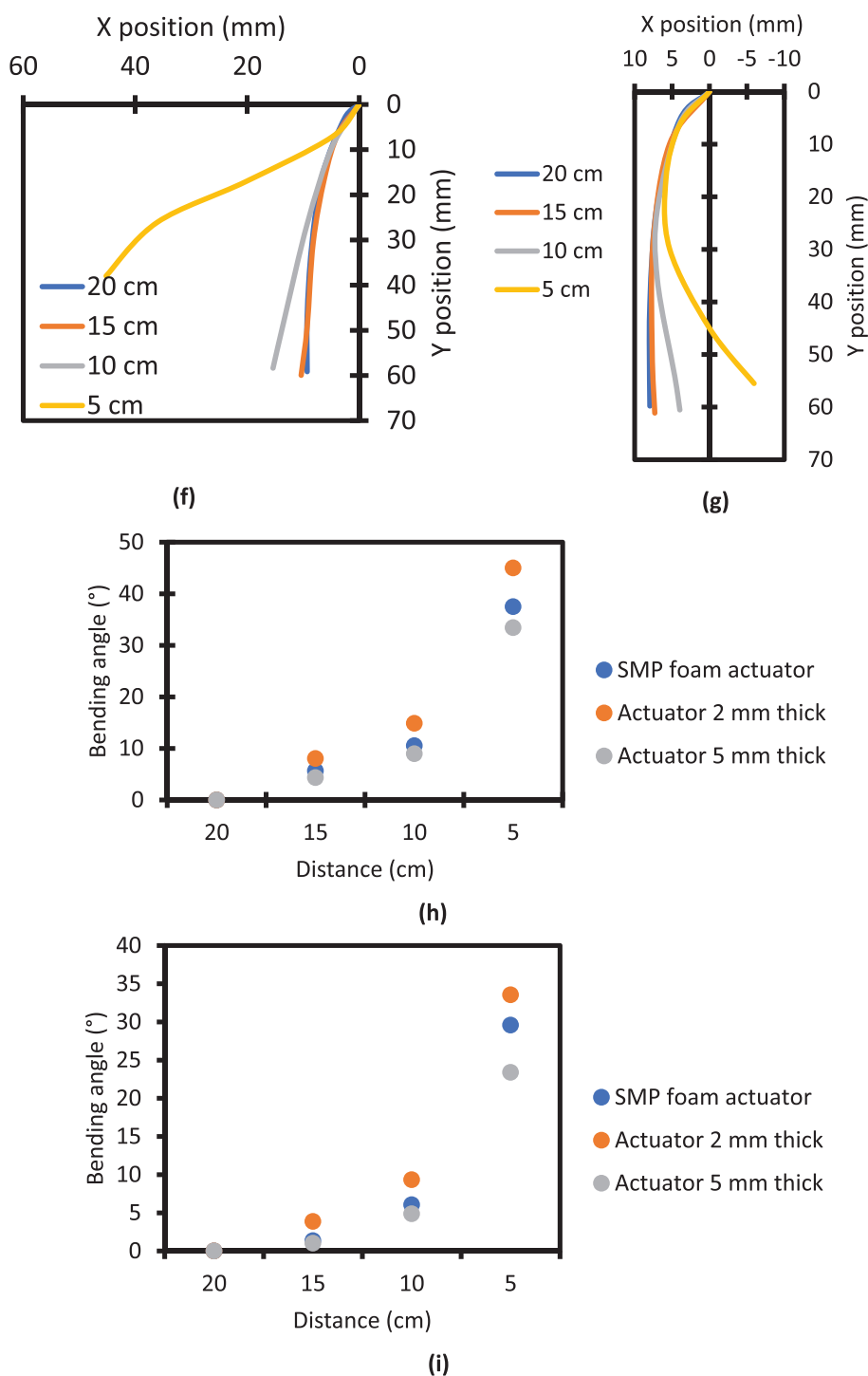


Figure 8. Continued

shapes up to 25 g which is more than its weight if the magnetic field presents (see Figure 10b). According to the trials, if an external field of 25 mT is supplied, the gripper can lift things that are eight times heavier than its own weight (3 g). As long as there is a magnet with a low field strength field, the gripper is able to hold

the object due to the friction between SMP and the object. The gripper is able to grasp and hold objects horizontally as shown in Figure 10c. However, the weight of objects should be the same or less than the actuator. The gripper cannot hold objects heavier than its weight in horizontal direction. However, this can be tack-

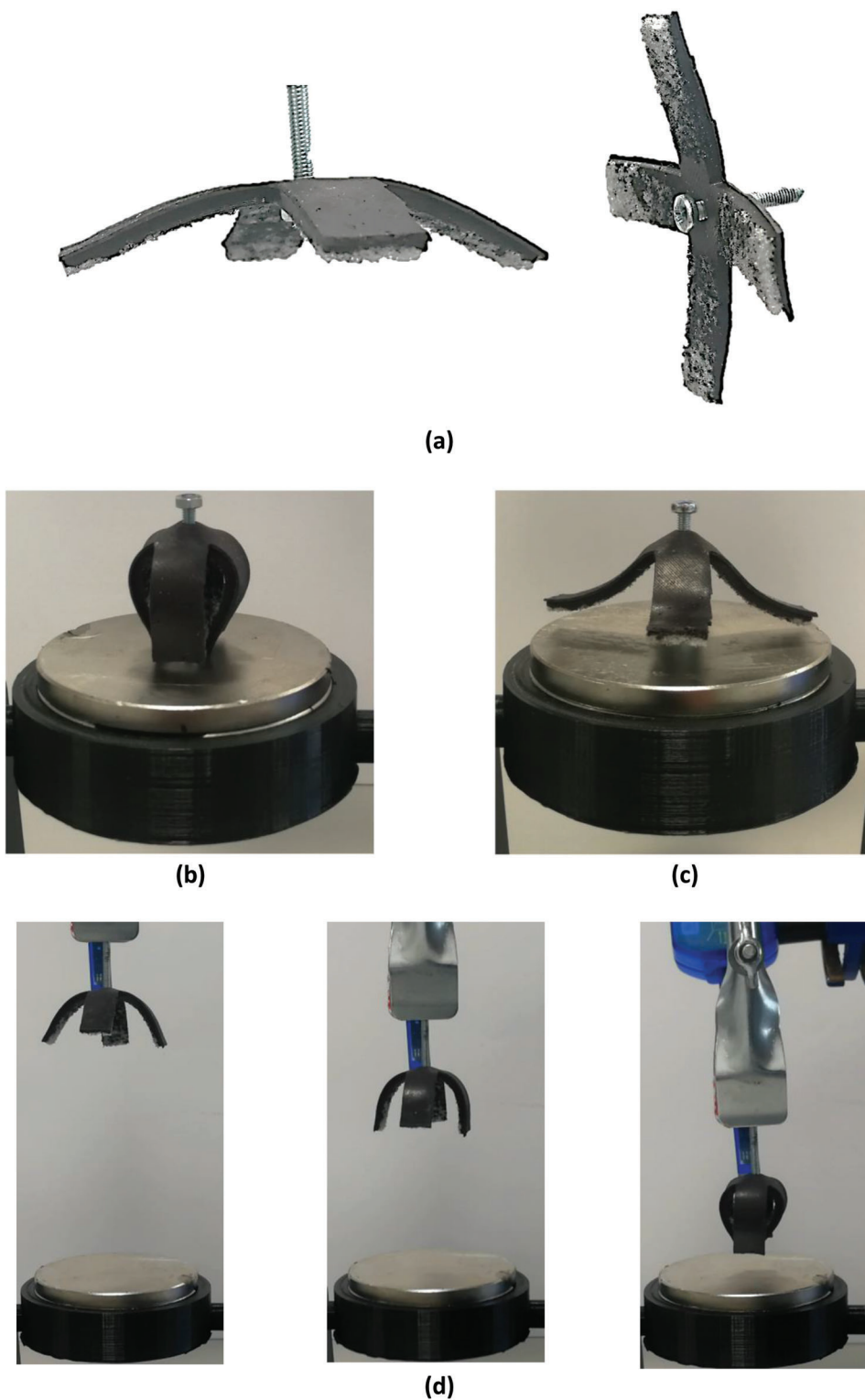


Figure 9. a) Composite actuator holding in vertical direction (left) and horizontal direction (right). Actuator's arms b) attraction and c) repulsion with 50 mT field strength. d) Gripper's arms retraction step by step by opposing 6 mT (left), 15 mT (middle), and 35 mT (right) external fields.

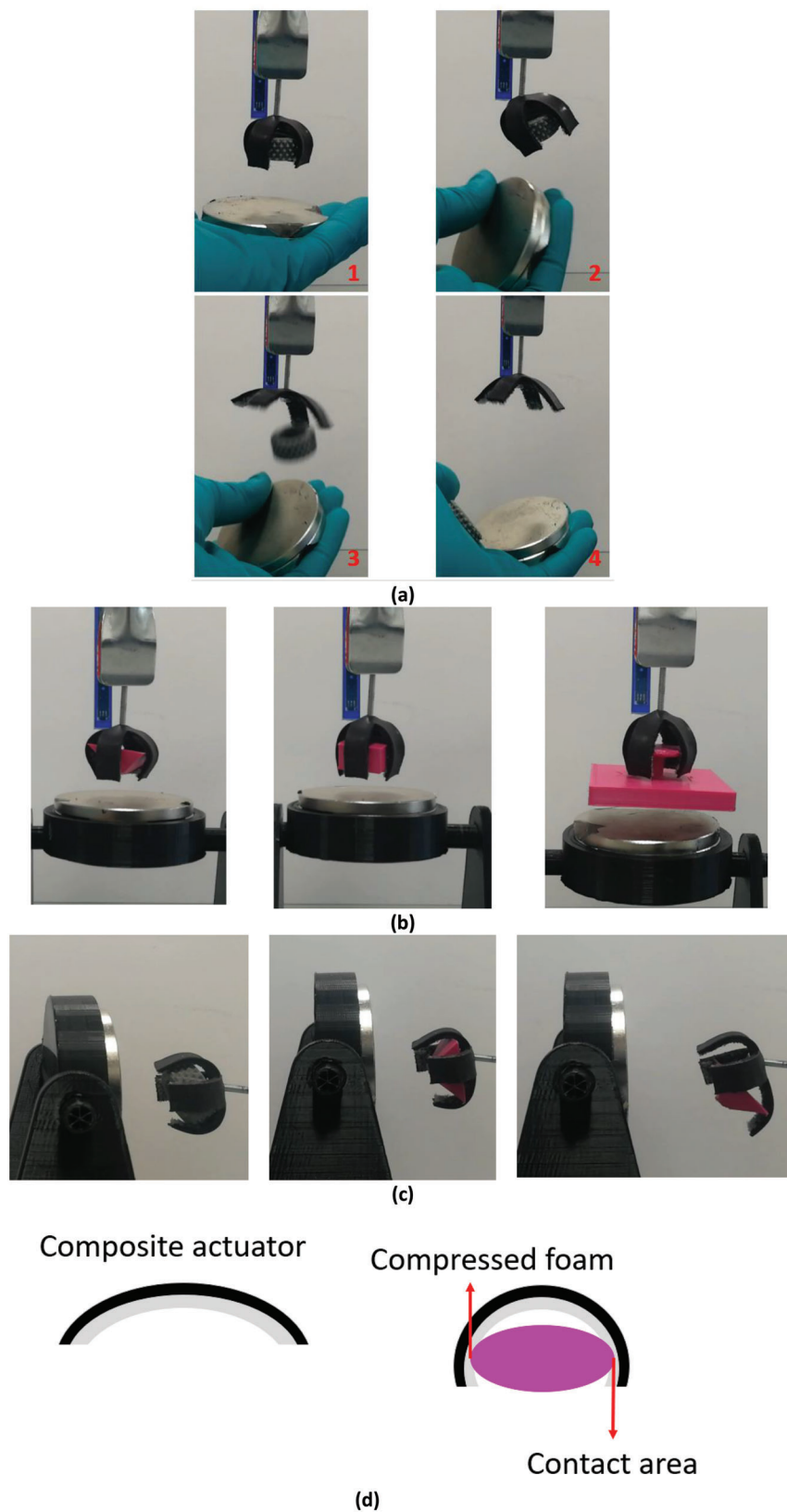


Figure 10. a) Steps of Holding and releasing the object (1.57 g) by rotating the magnet. b) Lifting and holding objects (2.92 g left, 4.57 g middle, and 25.63 g right) with different shapes in vertical direction. c) Holding and releasing the objects in horizontal direction. d) The schematic of the actuator grasping the object.

led by a stronger magnetic field. This is due to the stability that SMP provides throughout the gripper. The SMP foam does not let the magnetic elastomer hang and it holds the elastomer properly in the horizontal position. This helps the actuator to grasp the object easily which cannot be done without SMP foam. SMP foam improves the repeatability and controllability of the actuator without increasing the weight. The capacity of soft fingertips to offer contact area aids in deft grabbing, stability, and delicate object manipulation when gripping anything.

The results presented in Figures 9 and 10 have proved that the bi-directional gripper improves the holding and releasing of objects. The external field's induction of an outstretched arm conformation increases the contact force with the object to be held and leaves the bottom of the gripper open to allow for gentle sliding of the object during releasing (see Figure 10d). The contact areas between foam and object result in compressing shape-memory foam due to the generated force. This improves the ability of the composite actuator to hold objects. As soon as the actuator releases the object, the SMP foam goes back to its initial form. This study shows how a stable actuator can be controlled using a low magnetic field. Lifting and controlling the gripper may also be accomplished by utilizing larger external fields, provided that longer holding times and controlling the gripper from a long distance. Also, a fast response can be achieved by using a strong field. The method can be used to design and develop various shapes based on requirements. The size of the gripper can be larger as well. However, a stronger magnetic field or bigger magnets is required to control the actuator remotely. Using SMP foam as a base structure improves the stability and controllability of the actuator.

4. Conclusion

In conclusion, by simply casting particle-filled silicone resins, followed by SMP foam and controlled magnetization using commercial permanent magnets, it was possible to create shape-memory magneto-responsive soft composite actuators that are conformal, stable, and inexpensive. The actuator could be controlled with low magnetic field strength. The novel SMP foam was investigated in terms of microstructure, energy absorption, and reversibility (room-temperature shape recovery). It was founded that the SMP was fast enough to recover its original shape quickly under cycling loads and bending at room temperature. The microstructure, size, and shape of the magnetic particles and SMP foam were studied accordingly. This research showed how SMP foam could increase the contact force with a small area, the stability of thin magnetic elastomers, and reduce their weight as well. The SMP foam had a significant impact on the amount of magnetism attained after manufacturing. The results showed low field was required to actuate the composite actuator. Also, a bi-directional actuator was achieved by using a cubic shape magnet at the end of the composite film during curing. The maximum bending angle of 37° with a low external field of 17 mT was achieved for the SMP foam actuator. One of the applications of this soft composite actuator was shown in this study as a bi-directional soft gripper with high contact area and stability to operate in vertical and horizontal directions. This research is likely to advance the state-of-the-art soft actuation and unlock potentials in the design and development of composite magneto-

responsive soft actuators for different applications in roboticists, architects, packaging, and bioengineering as it follows a straightforward procedure, and requires inexpensive magnets and raw materials.

Acknowledgements

The authors gratefully acknowledge use of the services and facilities at Nottingham Trent University.

Conflict of Interest

The authors declare no conflict of interest.

Data Availability Statement

All data are included in the paper.

Keywords

composite actuators, magnetic composites, shape memory polyurethane foams, silicone resins, soft actuators

Received: July 23, 2022
Revised: August 11, 2022
Published online:

- [1] C. Majidi, *Adv. Mater. Technol.* **2018**, *4*, 1800477.
- [2] M. S. Xavier, C. D. Tawk, A. Zolfagharian, J. Pinski, D. Howard, T. Young, J. Lai, S. M. Harrison, Y. K. Yong, M. Bodaghi, A. J. Fleming, *IEEE Access* **2022**, *10*, 59442.
- [3] J. Xiong, J. Chen, P. S. Lee, *Adv. Mater.* **2021**, *33*, 2002640.
- [4] W. Dou, G. Zhong, J. Cao, Z. Shi, B. Peng, L. Jiang, *Adv. Mater. Technol.* **2021**, *6*, 2100018.
- [5] L. N. Awad, P. Kudzia, D. A. Revi, T. D. Ellis, C. J. Walsh, *IEEE Open J. Eng. Med. Biol.* **2020**, *1*, 108.
- [6] J. Rossiter, *Artif. Life Robot* **2021**, *26*, 269.
- [7] J. Wang, A. Chortos, *Adv. Intell. Syst.* **2022**, *4*, 2100165.
- [8] S. Y. Hann, H. Cui, M. Nowicki, L. G. Zhang, *Addit. Manuf.* **2020**, *36*, 101567.
- [9] X. Q. Shi, H. o L. Heung, Z. Q. Tang, Z. Li, K. Yu Tong, *J. Stroke Cerebrovasc. Dis.* **2021**, *30*, 105812.
- [10] W. Chen, B. Sun, P. Biehl, K. Zhang, *Macromol. Mater. Eng.* **2022**, *307*, 2200072.
- [11] H. Li, R. Li, K. Wang, Y. Hu, *Macromol. Mater. Eng.* **2021**, *306*, 2100166.
- [12] N. Bira, P. Dhagat, J. R. Davidson, *Front. Robot. AI* **2020**, *7*, <https://doi.org/10.3389/frobt.2020.588391>.
- [13] L. Zheng, S. Handschuh-Wang, Z. Ye, B. Wang, *Appl. Mater. Today* **2022**, *27*, 101423.
- [14] L. Fang, T. Fang, X. Liu, S. Chen, C. Lu, Z. Xu, *Macromol. Mater. Eng.* **2016**, *301*, <https://doi.org/10.1002/mame.201600139>.
- [15] C. Chang, L. e Zhao, Z. Song, Y. Zhou, S. Yu, *Macromol. Mater. Eng.* **2022**, *307*, 2100638.
- [16] E. Yarali, M. Baniyadi, A. Zolfagharian, M. Chavoshi, F. Arefi, M. Hossain, A. Bastola, M. Ansari, A. Foyouzat, A. Dabbagh, M. Ebrahimi, M. J. Mirzaali, M. Bodaghi, *Appl. Mater. Today* **2022**, *26*, 101306.

- [17] H.-Q. Tao, De.-W. Yue, C.-H. Li, *Macromol. Mater. Eng.* **2022**, *307*, 2100649.
- [18] W. Sang, L. Zhao, R. Tang, Y. Wu, C. Zhu, J. Liu, *Macromol. Mater. Eng.* **2017**, *302*, 1700239.
- [19] Y. Kim, G. A. Parada, S. Liu, X. Zhao, *Sci. Rob.* **2019**, *4*, <https://doi.org/10.1126/SCIROBOTICS.AAX7329>.
- [20] H. - W. Huang, M. S. Sakar, A. J. Petruska, S. Pané, B. J. Nelson, *Nat. Commun.* **2016**, *7*, <https://doi.org/10.1038/ncomms12263>.
- [21] C. Peters, O. Ergeneman, P. D. W. García, M. Müller, S. Pané, B. J. Nelson, C. Hierold, *Adv. Funct. Mater.* **2014**, *24*, 5269.
- [22] M. Stingaciu, A. Z. Eikeland, F. H. Gjørup, S. Deledda, M. Christensen, *RSC Adv.* **2019**, *9*, 12968.
- [23] J. A. Carpenter, T. B. Eberle, S. Schuerle, A. Rafsanjani, A. R. Studart, *Adv. Intell. Syst.* **2021**, *3*, 2000283.
- [24] S. Qi, H. Guo, J. Fu, Y. Xie, M. i Zhu, M. Yu, *Compos. Sci. Technol.* **2020**, *188*, <https://doi.org/10.1016/j.compscitech.2019.107973>.
- [25] Y. Ju, R. Hu, Y. Xie, J. Yao, X. Li, Y. Lv, X. Han, Q. Cao, L. Li, *Nano Energy* **2021**, *87*, 106169.
- [26] Y. Liu, H. Du, L. Liu, J. Leng, *Smart Mater. Struct.* **2014**, *23*, .
- [27] C. Du, J. Liu, D. A. Fikhman, K. S. Dong, M. B. B. Monroe, *Front. Bioeng. Biotechnol.* **2022**, *10*, <https://doi.org/10.3389/fbioe.2022.809361>.
- [28] G. Li, M. John, *Compos. Sci. Technol.* **2008**, *68*, 3337.
- [29] S. M. Hasan, L. D. Nash, D. J. Maitland, *J. Polym. Sci., Part B: Polym. Phys.* **2016**, *54*, <https://doi.org/10.1002/polb.23982>.
- [30] G. Li, D. Nettles, *Polymer (Guildf)*. **2010**, *51*, <https://doi.org/10.1016/j.polymer.2009.12.002>.
- [31] W.e Xu, G. Li, *Int. J. Solids Struct.* **2010**, *47*, 1306.
- [32] M. C. Boyce, G. G. Weber, D. M. Parks, *J. Mech. Phys. Solids* **1989**, *37*, 647.
- [33] H. R. Jarrah, A. Zolfagharian, R. Hedayati, A. Serjouei, M. Bodaghi, *Actuators* **2021**, *10*, 46.
- [34] A. Kausar, *Polym.-Plast. Technol. Eng.* **2018**, *57*, 346.
- [35] L. Santo, D. Santoro, F. Quadrini, (Eds. M. R. Maurya, K. K. Sadasivuni, J.-J. Cabibihan, S. Ahmad, S. Kazim), *Shape Memory Composites Based on Polymers and Metals for 4D Printing: Processes, Applications and Challenges*, Springer International Publishing, Cham, **2022**, https://doi.org/10.1007/978-3-030-94114-7_13.
- [36] B. C. Mac Murray, C. C. Futran, J. Lee, K. W. O'brien, A. A. Amiri Moghadam, B. Mosadegh, M. N. Silberstein, J. K. Min, R. F. Shepherd, *Soft Rob.* **2018**, *5*, 99.
- [37] C. M. Donatelli, Z. T. Serlin, P. Echols-Jones, A. E. Scibelli, A. Cohen, J. - M. Musca, S. Rozen-Levy, D. Buckingham, R. White, B. A. Trimmer, *IEEE/RSJ International Conference on Intelligent Robots and Systems (IROS)*, IEEE, Piscataway, NJ **2017**, <https://doi.org/10.1109/IROS.2017.8202196>.
- [38] N. Kastor, R. Mukherjee, E. Cohen, V. Vikas, B. A. Trimmer, R. D. White, *Robotica* **2020**, *38*, 88.
- [39] H. Tripathi, G. C. Pandey, A. Dubey, S. K. Shaw, N. K. Prasad, S. P. Singh, C. Rath, *Adv. Eng. Mater.* **2021**, *23*, 2000275..
- [40] A. De Oliveira Barros, M.d N. Hasan Kashem, D. Luna, W. J. Geerts, W. Li, J. Yang, *AIP Adv.* **2022**, *12*, 035121.
- [41] M. Lalegani Dezaki, M. K. A. Mohd Ariffin, S. Hatami, *Rapid Prototyping J.* **2021**, *27*, 562.
- [42] N. N. Azmi, M. N. A. Ab Patar, S. N. A. Mohd Noor, J. Mahmud, *International Symposium on Technology Management and Emerging Technologies*, IEEE, Piscataway, NJ **2014**, <https://doi.org/10.1109/ISTMET.2014.6936529>.
- [43] N. A. Algarou, Y. Slimani, M. A. Almessiere, S. Rehman, M. Younas, B. Unal, A. D. Korkmaz, M. A. Gondal, A. V. Trukhanov, A. Baykal, I. Nahvi, *J. Taiwan Inst. Chem. Eng.* **2020**, *113*, 344.
- [44] H. Wang, L. Xu, C. Liu, Z. Jiang, Q. i Feng, T. Wu, R. Wang, *Ceram. Int.* **2020**, *46*, 460.
- [45] S. Chen, Y. Di, H. Li, M. Wang, B. i Jia, R. Xu, X. Liu, *Appl. Surf. Sci.* **2021**, *559*, 149855.